On the Radiation Fields of Fast Radio Bursts Close to Sources

Yu Zhang and Hui-Chun Wu*
Institute for Fusion Theory and Simulation and Department of Physics, Zhejiang University, Hangzhou 310027, China
(Dated: November 22, 2021)

Fast radio bursts (FRBs) are coherent powerful radio transients with cosmological origins. The detected galactic FRB reveals that magnetars can generate FRBs, however the mechanism still remains enigmatic. Characteristics of FRBs are limited to observable quantities such as luminosity, duration, spectrum and repetition etc. Due to the uncertainties of triggering mechanisms and source sites within or out of magnetospheres of neutron stars, status of FRBs close to their sources are unknown. As an extreme astronomical event, FRBs could accompany with energy-comparable or even more powerful x/γ-ray counterparts. Here, we study the interaction of ultrastrong radio pulses in GHz and high-energy photons in GeV. Particle-in-cell simulations show that at the field-strength of about 3×10^{12}V/cm, quantum cascade effects can generate dense pair plasmas and the radio pulses are significantly depleted. Therefore, GHz radio pulses of stronger than 3×10^{12}V/cm is difficult to escape from emitters if accompanying with GeV photons. This process could afford a limit to the FRB field strength nearby sources. Investigation on the toleration of $\gtrsim 10^{12}$V/cm radio waves for potential plasma/beam emitters in neutron-star scenerios should be helpful to distinguish the precise mechanism of FRBs.

Since first discovered in 2007 [1], fast radio bursts (FRBs) had been recognized as real astronomical events and gained intense research [2–4]. Although event reports and theoretical models on the FRBs have exploded for one decade, the origin of FRBs still remains enigmatic. Due to large dispersion measures with hundreds or even thousands of cm^{-3}pc, these radio transients have cosmological origins [5], which has been confirmed by several events with located host galaxies [6, 7]. Now FRBs have served as novel probes for interstellar and intergalactic matters [8, 9].

Assuming an isotropic emission, the luminosity of FRBs ranges from10^{38} to10^{45}erg/s [6, 10], many orders of magnitude powerful than radio pulsars. Meanwhile, the ultrahigh brightness temperature $\sim 10^{35}$K [2, 4] indicates that FRB radiations must be coherent. The millisecond duration implies that the source scale is limited to hundreds of kilometers, which points to the compact objects, such as white dwarfs, neutron stars or black holes. Recently, the observed FRB200428 [11–13] in the Milky Way associates with a hard X-ray burst from magnetar SGR1935+2154, which establishes that magnetars can generate FRBs.

Many models [2–4] have been proposed for FRBs. For the models employing solitary neutron stars, possible FRB sources are located within or out of magnetospheres surrounding neutron stars. In the magnetosphere, the radiation mechanisms have plasma maser emissions from relativistic plasmas or plasma instabilities [14], and curvature radiation of charged bunches [15–18]. Outside of magnetosphere, relativistic shocks driven by outflows from neutron stars may also induce FRBs [19–22]. Therefore, the emission region of FRBs from neutron stars is still debated. However, it is common that these models predict that FRBs are accompanied with energy-comparable or even much more powerful counterparts in x/gamma-ray bands of keV to TeV [23]. The observed x-rays from FRB200428 are about four orders of magnitide more energetic than the radio emission.

FRBs have been detected in range of 0.3-8 GHz [4] with a bandwidth of hunderds of MHz limited by the detection band of radio telescopes. The coherent GHz radiation implies an emitter in sub-meter scale. In the immediate vicinity of the emitters, the FRB is an extremely strong microwave. Research on this extreme microwave is rare [24]. Here, we simulate the interaction between ultrastrong radio waves in GHz and gamma photons in GeV, and find that at the field-strength about 3×10^{12}V/cm, dense pair plasmas are produced by quantum cascades and significantly damp the radio pulses. This process should occur in the FRB emission region and constrains the radiation intensity near the emitters.

First, let us roughly estimate the FRB field strength near the source. The FRB energy can be expressed as $W = d\Omega \cdot R^2 \cdot cT \cdot \varepsilon_0 E^2$, where $d\Omega$ is the solid angle of the FRB emission cone, E is the field amplitude at a distance R from the source, $T \approx 1$ms is the duration, c is the light speed, and ε_0 is the vacuum permittivity. For the isotropic emssion assumption $d\Omega = 4\pi$, the estimated energy range is $W_i = 10^{35} \sim 10^{42}$erg. So the field strength E can be obtained from

$$W_i = 4\pi R^2 \cdot cT \cdot \varepsilon_0 E^2 \tag{1}$$

The blue block in Fig. 1 shows the possible E range as a function of R. The field strength range is $1.7 \times 10^9 \sim 5.4 \times 10^{12}$V/cm for $R = 100$ km. The solid line marks the Schwinger field $E_s = 1.32 \times 10^{16}$V/cm. The dashed line is the critical field strength 3×10^{12}V/cm revealed in our simulations, where high-energy photons can trigger strong quantum cascades and radiation damping. For a point source, E in Eq. (1) will diverge when $R \to 0$.

*huichunwu@zju.edu.cn

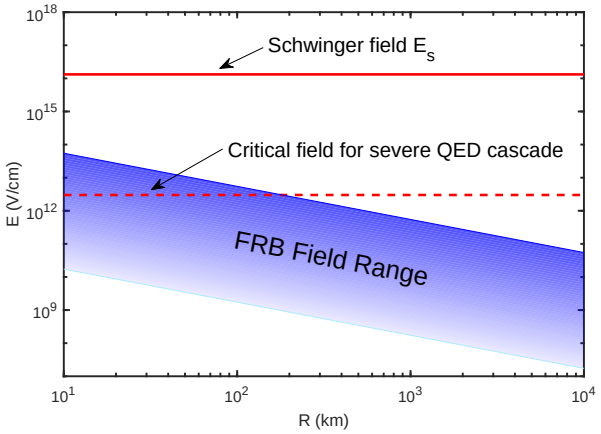

FIG. 1: Estimated FRB field strength E as a function of the distance R from sources.

The actural emisson zone should consist of many emitters and have a total emission surface with the area of S. The emission energy has $W = S \cdot cT \cdot \varepsilon_0 E^2$, similar to Eq. (1). For $S = 10^5 \mathrm{km}^2$, one has $E = 1.95 \times 10^9 \sim 6.14 \times 10^{12} \mathrm{V/cm}$.

We use the code JPIC1d-QED to simulate the interaction between ultra-strong FRBs and gamma photons. To simulate the avalanche of positron-electron pairs, two quantum electrodynamics (QED) effects, the Breit-Wheeler process and the nonlinear inverse Compton scattering [25–27] are embed into the one-dimensional (1D) particle-in-cell (PIC) code JPIC1d [28]. Production of positron-electron pairs and photons are determined by the Monte-Carlo algorithm with their respective quantum generation rates [25, 29, 30]. A particle-merging scheme is adopted to deal with rapidly increased particles in the avalanche. To suppress numerical noises typically encountered in PIC-QED simulations, we adopt the five-point particle interpolation for positrons/electrons. Our code has done the benchmark for single-electron quantum cascades in a static magnetic field [25, 31] and repeated the results of ultraintense laser QED breakdowns triggered by a single electron [30].

The Breit-Wheeler process generates electron-positron pairs by the annihilation of gamma photons in electromagnetic fields. The inverse Compton scattering describes gamma photon emission by relativistic electrons/positrons accelerated by FRB fields. Both effects are measured by the following term (SI units)

$$\chi \simeq \frac{\gamma}{E_s}\sqrt{(\boldsymbol{E} + \boldsymbol{v} \times \boldsymbol{B})^2 - (\boldsymbol{v} \cdot \boldsymbol{E})^2/c^2} \qquad (2)$$

Here γ is the Lorentz factors of electrons/positrons and photons, $\boldsymbol{v}$ is the particle speed, $\boldsymbol{E}$ and $\boldsymbol{B}$ are the electric and magnetic fields respectively. For photons, one has $\gamma = \epsilon/mc^2$ and $|\boldsymbol{v}| = c$, ϵ is the photon energy, m is the electron rest mass. Obvious QED cascades occurs at $\chi \simeq 0.1$, and massive particles and photons emit when $\chi \to 1$.

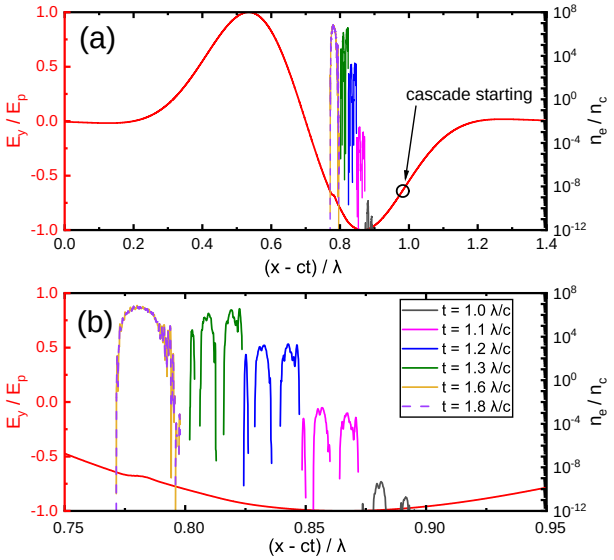

FIG. 2: (a) Evolution of electron density n_e in the comoving frame of the electric field E_y. Positron density is the same as the electron density. (b) Zooming in on the electron densities n_e in (a).

Hundreds of MHz bandwidth imply the coherent time of a few nanoseconds, and therefore millisecond FRBs should consist of many coherent nanosecond subpulses. We are going to study the interaction between this nanosecond subpulse and gamma photons. We attempt to find the critical field strength for significant quantum cascades within the subcycle of radio waves. Dense pair plasmas generated in the subcycle can damp a significant portion of the entire multiple-cycle pulse [30]. Since FRBs are highly polarized, we take a bipolar waveform $E_y = E_0 \exp(-t^2/\tau^2)\sin(\omega_0 t)$ in simulations, where the central frequency $\omega_0/2\pi = 1\mathrm{GHz}$, and $\tau = 0.3\lambda/c$ with the wavelength $\lambda \approx 30\mathrm{cm}$. This radio pulse propagates along the x axis and has the peak field strength $E_p = 0.636 \cdot E_0$ due to the carrier-envelope phase effect.

Although TeV radiations are also predicted for FRB events, we mainly focus on the GeV-level triggering particles, which is not a rigorous requirement for extreme environments in neutron stars [32]. Quantum cascades are sensitive to the interaction angle between fields and particles. From Eq. (2), one can obtain

$$\chi \simeq \frac{\gamma}{E_s}(E_y - v_x B_z) = \frac{\gamma E_y}{E_s}(1 - \frac{v}{c}\cos\theta) \qquad (3)$$

where θ is the separation angle between the particle velocity $\boldsymbol{v}$ and the x axis. It is obvious that the QED effects are negligible for $\theta = 0°$ and efficient for a head-on collision with $\theta = 180°$. For $\gamma = 2000$ and $\theta = 180°$, the field strength for obvious quantum cascades at $\chi = 0.1$ is $E = 3.3 \times 10^{11} \mathrm{V/cm}$.

Both particles and photons seem to be equivalent to trigger quantum cascades. However, due to strong field

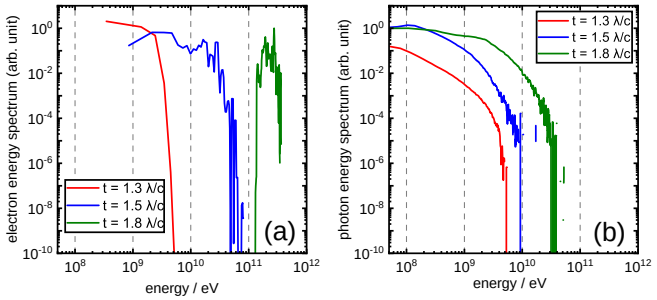

FIG. 3: Electron energy spectra (a) and photon energy spectra (b) at $t = 1.3\lambda/c$, $1.5\lambda/c$ and $1.8\lambda/c$. Positrons have the almost same energy spectrum as electrons.

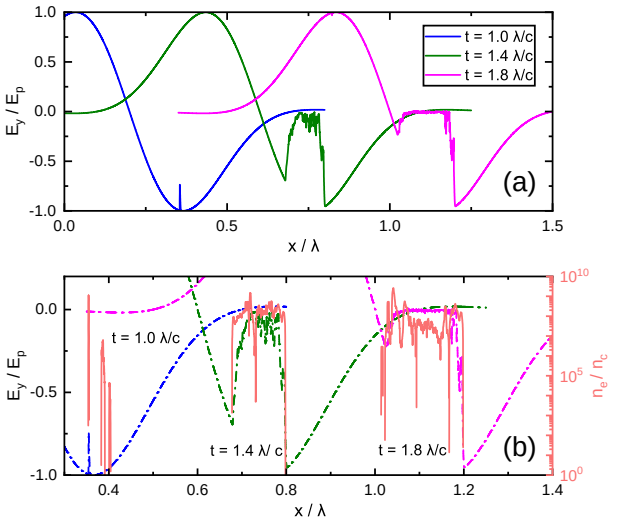

FIG. 4: (a) Evolution of the electric field E_y in the real space at $t = 1\lambda/c$, $1.4\lambda/c$ and $1.8\lambda/c$. (b) Zooming in on the field E_y in (a) and the electron density n_e of pair plasmas. Here the dashed and solid lines represent the field and electron density, respectively.

interaction, charged particles in GeV are difficult to trigger quantum cascades in FRB fields. The colliding electrons/positrons will be decelerated in the longitudinal direction by the ultrastrong phonderomotive force of FRB fields, and then turn back and copropagate with the fields at $\theta \approx 0$, where QED effects are inefficient. This kind of reflection within the FRB fields occurs for the incident particle energy smaller than $\gamma_{rf} \approx a_0/4$ [33], where $a_0 = eE/mc\omega_0$ is the normalized field. For 1 GHz radio waves with $E = 3.3 \times 10^{11}$V/cm, one has $a_0 = 3.1 \times 10^6$ and $\gamma_{rf} \approx 7.8 \times 10^5$, i.e. 0.4 TeV. If high-energy electrons can get the chance to emit gamma photons, quantum cascades are possible because these gamma photons can freely penetrate into the strong FRB fields and annihilate into electron-positron pairs.

The first simulation is done for $E_p = 2.68 \times 10^{12}$V/cm, which corresponds to $a_0 = eE_p/m_e c\omega_0 \simeq 2.5 \times 10^7$ and the magnetic field of $E_p/c \simeq 0.89 \times 10^{10}$Gauss. The simulation box is 2λ length with the spatio-temporal resolution of 10000 grids per wavelength/cycle. Ten photons at 1 GeV are simultaneously incident to the FRB pulse with $\theta = 120°$.

Figure 2 shows photon-triggered pair plasma sparks in the comoving-frame of the radio pulse. Obvious QED cascades occur at $E_y \approx 0.7E_{p0}$, where the incident photons have annihilated and hundreds of pairs appears with the local factor $\chi \approx 0.1$. These electrons/positrons are then accelerated violently by the FRB field to ultrarelativisitic energies and emit high-energy photons, which further annihilate into electron-positron pairs. As shown in Fig. 2, three distinct plasma clumps appear, grow and finally merge into a plasma sheet within the period of $\sim$ 1 ns. The plasma density increases exponentially before the clump merging and saturates at $t = 1.6\lambda/c$ with the peak density of $7.2 \times 10^6 n_c$. Here, $n_c \simeq 1 \times 10^{13}(\mathrm{cm}/\lambda)^2\mathrm{cm}^{-3} = 1.11 \times 10^{10}\mathrm{cm}^{-3}$ is the critical density for 1 GHz waves. After $t = 1.6\lambda/c$, the pair plasma sheet co-moves with the field, and hence quantum cascades cease. For an ultra-relativistic field, the plasma density for screening the field is approximately given by $a_0 n_c$. The plasma sheet has a density lower than $a_0 n_c = 2.5 \times 10^7 n_c$ and is thin as 0.01λ, and so it only causes a slight distortion on the FRB field.

Figure 3 shows the energy spectra of electrons and photons. During the active cascades, particles and photons are stimulated with each other and have the almost same maximum energy, as shown at $t = 1.3\lambda/c$. Due to the highfield acceleration, the charged particles are always more concentrated in energy than photons. After the saturation, the charged particles are free of radiation damping, and their energy quickly surpass that of photons (see the moment $t = 1.5\lambda/c$). Pair plasmas are accelerated to be monoenergetic with an average energy$\sim$ 0.2 TeV at $t = 1.8\lambda/c$.

We increase the peak field strength to $E_p = 3 \times 10^{12}$ V/cm with $a_0 = 2.8 \times 10^7$. Figure 4 shows the electric field E_y and pair plasma density n_e in the real space. Due to generated pair plasmas, partial field screening starts at $t \approx 1\lambda/c$. Then, the plasma density dramatically increases and exceeds the relativistic critical density $a_0 n_c \approx 2.8 \times 10^7 n_c$. The field screening is complete with a null field in the plasma with $n_e > a_0 n_c$. After the complete field screening, the pair plasma expands towards the frontside and further grows to the backside. Figure 5 shows the distribution of electron energies in the space. On the front of the plasma, electrons/positrons are further accelerated to higher energies with momentum dominantly along the x axis. The QED effects are weak according to Eq. (3) and pairs are not produced anymore. On the backside, oscillating charged particles on the vaccum-plasma boundary continues to collide with the right-going field and produce new pairs. Due to the continuous radiation damping, these particles are suppressed in energy as shown in Fig. 5(b,c), compared to accelerated particles on the right front. In Fig. 5(c), one can notice that a plasma spark appears downstream in the second half cycle and is triggered by the emitted

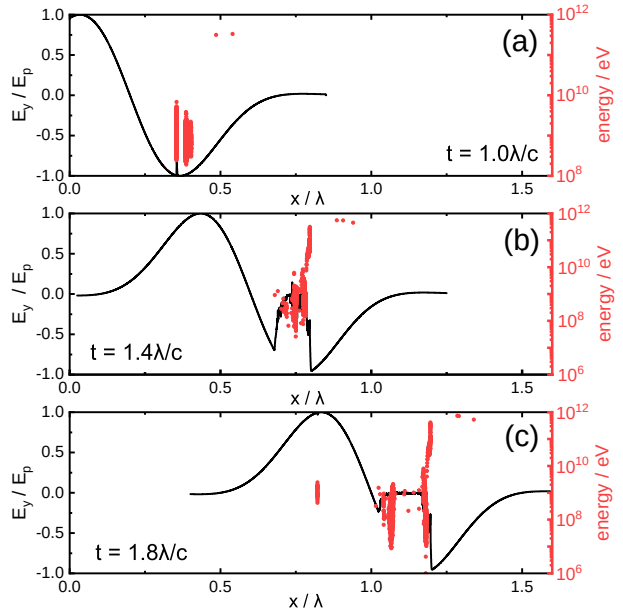

FIG. 5: Electron energy distribution superposed with the field at the moments (a) $t = 1\lambda/c$, (b) $t = 1.4\lambda/c$ and (c) $t = 1.8\lambda/c$.

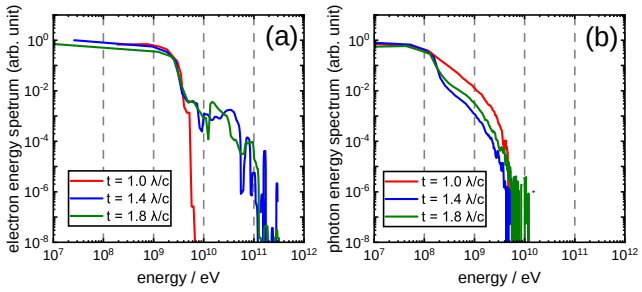

FIG. 6: Electron energy spectra (a) and photon energy spectra (b) at $t = 1\lambda/c$, $1.4\lambda/c$ and $1.8\lambda/c$.

photons from the QED-active backside of the pair plasma block. This spark could damp the FRB field in the more extended space.

Energy spectra of electrons and photons are given in Fig. 6. During the active quantum cascades at $t = 1\lambda/c$, charged particles and photons have the similar spectra same as the case in Fig. 3. After the complete field screening, the high-energy part of the spectra at $t = 1.4\lambda/c$ and $1.8\lambda/c$ in Fig. 6(a) comes from particles due to the field acceleration at the plasma front. Depletion of GeV photons from $t = 1\lambda/c$ to $1.4\lambda/c$ is due to the significant materialization of pair plasmas by the photon annihilation.

Gamma photons of above 1 GeV are observed to more easily lead to the above results in Fig. 4. We also carry out the simulations for charged particles in GeV-TeV, and find that tens of GeV are requested to trigger significant radiation damping due to the strong field-particle interaction discussed before.In the 3D space, pair plasmas should occupy the main volume of the radio fields as demonstrated in multi-dimentional PIC simulation of ultraintense laser breakdown in vacuum [30] triggered by a single electron.On the other hand, we only adopt tens of photons incident to the FRB fields. According to the different FRB models, GeV-TeV photons with a comparable energy as radio emission are possible to co-exist with FRBs. These huge amount of high-energy photons will deplete the whole FRBs.

To conclude, we investigate radiation dampings of FRBs triggered by accomponying higher-energy photons in GeV. At the field amplitude of 3.0×10^{12}V/cm, dense pair plasmas are generated within sub-cycle of these radio transients. Plasma materialization and radiation absorption lead to the breakdown of FRBs fields. This important energy-depletion mechanism could critically limit the field-strength of FRBs around their emitters. Our work also implies that QED effects [34, 35] could be indispensable for the FRB emitter.

Acknowledgments

This work was supported by the Strategic Priority Research Program of Chinese Academy of Sciences (Grant No.XDA17040503). We thank W. M. Wang for helpful discussions.

[1] D. R. Lorimer *et al.*, Science **318**, 777 (2007).
[2] J. I. Katz, Prog. Part. Nucl. Phys. **103**, 1 (2018).
[3] E. Platts *et al*, Phys. Rep. **821**, 1 (2019).
[4] B. Zhang, Nature **587**, 45 (2020).
[5] J. Xu and J. L. Han, Res. Astron. Astrophys. **15**, 1629 (2015).
[6] D. Thornton *et al.*, Science **341**, 53 (2013).
[7] E. Petroff *et al.*, Publ. Astron. Soc. Aust **33**, e045 (2016).
[8] J. X. Prochaska *et al.*, Science **366**, 231 (2019).
[9] J. P. Macquart *et al.*, Nature **581**, 391 (2020).
[10] B. Zhang, Astrophys. J. Lett. **867**, L21 (2018).
[11] C. D. Bochenek *et al*, Nature **587**,59 (2020).
[12] B. C. Andersen *et al*, Nature **587**, 54 (2020).
[13] L. Lin *et al.*, Nature **587**, 63 (2020).
[14] Y. Lyubarsky, Astrophys. J. **897**, 1 (2020).
[15] P. Kumar, W. B. Lu, and M. Bhattacharya, Mon. Not. R. Astron. Soc **468**, 2726 (2017).
[16] J. I. Katz, Phys Rev D **89**, 103009 (2014).
[17] Y. P. Yang, J. P. Zhu, B. Zhang, and X. F. Wu, Astrophys. J. Lett. **901**, L13 (2020).
[18] W. B. Lu and P. Kumar, Mon. Not. R. Astron. Soc. **477**, 2457 (2018).
[19] Y. Lyubarsky, Mon. Not. R. Astron. Soc. **442**, L9 (2014).
[20] E. Waxman, Astrophys. J. **842**, 34 (2017).

[21] B. D. Metzger, B. Margalit, and L. Sironi, Mon. Not. R. Astron. Soc. **485**, 4091 (2019).
[22] A. M. Beloborodov, Astrophys. J. **896**, 142 (2020).
[23] G. Chen, V. Ravi, and W. B. Lu, Astrophys. J. **897**, 146 (2020).
[24] H.-C. Wu, Sci. Rep. **6**, 28263 (2016).
[25] N. V. Elkina *et al*, Phys. Rev. STAB **14**, 054401 (2011).
[26] T. Erber, Rev. Mod. Phys. **38**, 626 (1966).
[27] J. G. Kirk, A. R. Bell, and I. Arka, Plasma Phys. Controlled Fusion **51**, 085008 (2009).
[28] H.-C. Wu, arXiv: 1104.3163 (2011).
[29] W.-M. Wang *et al*, Phys. Rev. E **96**, 013201 (2017)
[30] E. N. Nerush *et al*, Phys. Rev. Lett. **106**, 035001 (2011)
[31] V. Anguelov and H. Vankov, J. Phys. G: Nucl. Part. Phys. **25**, 1755 (1999).
[32] W. Becker, *Neutron Stars And Pulsars* (Springer-Verlag, Berlin, 2009).
[33] H.-C. Wu *et al*, Phys. Rev. STAB. **14**.070702 (2011).
[34] A. Philippov, A. Timokhin, and A. Spitkovsky, Phy. Rev. Lett. **124**, 245101 (2020).
[35] J. I. Katz, Mon. Not. R. Astron. Soc. **469**, L39 (2017).